



Published in final edited form as:

*Bioorg Med Chem Lett.* 2007 December 15; 17(24): 6836–6840.

## Structure activity relationship study of [1,2,3]thiadiazole necroptosis inhibitors

Xin Teng<sup>a</sup>, Heather Keys<sup>b</sup>, Arumugasamy Jeevanandam<sup>c</sup>, John A. Porco Jr.<sup>c</sup>, Alexei Degterev<sup>b</sup>, Junying Yuan<sup>d</sup>, and Gregory D. Cuny<sup>\*,a</sup>

<sup>a</sup>Laboratory for Drug Discovery in Neurodegeneration, Harvard Center for Neurodegeneration and Repair, Brigham & Women's Hospital and Harvard Medical School, 65 Landsdowne Street, Cambridge, MA 02139, USA

<sup>b</sup>Department of Biochemistry, Tufts University Medical School, 136 Harrison Avenue, Stearns 703, Boston, MA 02111, USA

<sup>c</sup>Department of Chemistry, Boston University and Center for Chemical Methodology and Library Development (CMLD-BU), Boston, MA 02215, USA

<sup>d</sup>Department of Cell Biology, Harvard Medical School, 240 Longwood Avenue, Boston, MA 02115, USA

### Abstract

Necroptosis is a regulated caspase-independent cell death mechanism that results in morphological features resembling non-regulated necrosis. This form of cell death can be induced in an array of cell types in apoptotic deficient conditions with death receptor family ligands. A series of [1,2,3]thiadiazole benzylamides was found to be potent necroptosis inhibitors (called necrostatins). A structure activity relationship study revealed that small cyclic alkyl groups (i.e. cyclopropyl) and 2,6-dihalobenzylamides at the 4- and 5-positions of the [1,2,3]thiadiazole, respectively, were optimal. In addition, when a small alkyl group (i.e. methyl) was present on the benzylic position all the necroptosis inhibitory activity resided with the (*S*)-enantiomer. Finally, replacement of the [1,2,3]thiadiazole with a variety of thiophene derivatives was tolerated, although some erosion of potency was observed.

---

Cell death has traditionally been categorized as either apoptotic or necrotic based on morphological characteristics.<sup>1</sup> These two modes of cell death were also initially thought to fundamentally differ in underlying cellular regulation, with the former representing a regulated caspase-dependent mechanism,<sup>2</sup> while the latter resulting from non-regulated processes. However, more recent studies demonstrate that the underlying basis of cellular necrosis is more complex, as it can result in some instances from regulated caspase-independent cellular signaling.<sup>3</sup>

A regulated caspase-independent cell death pathway with morphological features resembling necrosis, called necroptosis, has recently been described.<sup>4</sup> This manner of cell death can be initiated with various stimuli (e.g. TNF- $\alpha$  and Fas ligand) and in an array of cell types (e.g. monocytes, fibroblasts, lymphocytes, macrophages, epithelial cells and neurons). Necroptosis may represent a significant contributor to and in some cases predominant mode of cellular

---

\*To whom correspondence should be addressed: Phone: +1-617-768-8640, Fax: +1-617-768-8606, E-mail: gcuny@rics.bwh.harvard.edu

**Publisher's Disclaimer:** This is a PDF file of an unedited manuscript that has been accepted for publication. As a service to our customers we are providing this early version of the manuscript. The manuscript will undergo copyediting, typesetting, and review of the resulting proof before it is published in its final citable form. Please note that during the production process errors may be discovered which could affect the content, and all legal disclaimers that apply to the journal pertain.

demise under pathological conditions involving excessive cell stress, rapid energy loss and massive oxidative species generation, where the highly energy-dependent apoptosis process is not operative. The discovery of necroptosis, therefore, raises the possibility of novel therapeutic intervention strategies for the treatment of maladies where necrosis is known to play a prominent role,<sup>5</sup> including organ ischemia (i.e. stroke<sup>6</sup> and myocardial infarction<sup>7</sup>), trauma and possibly some forms of neurodegeneration.<sup>8</sup>

The identification and optimization of low molecular weight molecules capable of inhibiting necroptosis will assist in elucidating its role in disease patho-physiology and could provide lead compounds (i.e. necrostatins) for therapeutic development. A series of hydantoin containing indole derivatives, exemplified by **1**, was the first potent *in vitro* and *in vivo* necroptosis inhibitors to be described (Figure 1).<sup>4,9</sup> Since then, a series of tricyclic derivatives, exemplified by **2**,<sup>10</sup> and substituted 3H-thieno[2,3-d]pyrimidin-4-ones, exemplified by **3**,<sup>11</sup> have also been reported. In the course of continued screening for additional classes of necroptosis inhibitors, we discovered that the [1,2,3]thiadiazole derivative **4** was a moderately potent inhibitor ( $EC_{50} = 1.0 \mu\text{M}$ ).<sup>12</sup> Herein, we report an initial structure activity relationship (SAR) study for this class of necroptosis inhibitors.

Many of the [1,2,3]thiadiazole derivatives evaluated herein were prepared according to the procedure outlined in Scheme 1. Meldrum's acid, **5**, was treated with acyl chlorides in the presence of pyridine to give  $\beta$ -ketoesters **6**.<sup>13</sup> The esters were allowed to react with mono-Boc-hydrazine in the presence of a catalytic amount of p-toluenesulfonic acid (p-TsOH) to give imines **7**.<sup>14</sup> Cyclization in the presence of thionyl chloride yielded the [1,2,3]thiadiazole esters **8**. Acid hydrolysis of the esters provided acids **9**. These materials were coupled with various amines utilizing HBTU (Method A), the corresponding acyl chlorides (Method B) or through the use of EDCI (Method C) to give amides **10**.

Compound **14** was prepared according to the procedure outlined in Scheme 2. Ester **11** was reduced with sodium borohydride to give **12**. The alcohol was converted to the corresponding aldehyde **13** utilizing Dess-Martin reagent. The aldehyde was condensed with 2-chloro-6-fluorobenzylamine in the presence of anhydrous magnesium sulfate to give an imine, which was subsequently used as crude material. The imine was then reduced with sodium triacetoxyborohydride to give the secondary amine **14**. The imide derivative **17** was also prepared starting with acid **15**, which was first converted to the corresponding acid chloride **16**. This material was then allowed to react with the anion of 2-chloro-6-fluorobenzamide generated with sodium hydride to give imide **17** in 34% yield.

The  $\alpha$ -substituted ( $\pm$ )-2-chloro-6-fluorobenzylamines were prepared according to Scheme 3. 2-Chloro-6-fluorobenzophenone, **18a**, was reduced with borane-THF complex to give the corresponding secondary alcohol. The alcohol was converted to the corresponding phthalimide via a Mitsunobu reaction followed by treatment with hydrazine monohydrate to give **19a**.<sup>15</sup> Nitriles **18b** and **18c** were treated with borane-THF complex followed by addition of *n*-BuLi or PhLi to give amines **19b** and **19c**, respectively.<sup>16</sup> The benzylnitrile **20a** was first dialkylated with methyl iodide to give **20b**. This material was hydrolyzed to the corresponding carboxylic acid and then subjected to a one-pot Curtius rearrangement (via an *in situ* generated acyl azide) to give a Boc-protected amine that upon deprotection yielded amine **21**.<sup>17</sup>

(*S*)-1-(2-Chloro-6-fluorophenyl)ethylamine was prepared by allowing **22** to react with methyl magnesium chloride followed by treatment with acetic anhydride to give  $\alpha$ -enamide **23** (Scheme 4). Asymmetric hydrogenation in the presence of the chiral catalyst (*S, S*)-Me-BPE-Rh gave amide **24**.<sup>18</sup> Acid hydrolysis of the amide yielded the optically pure amine **25**, isolated as the hydrochloride salt. Similarly, (*R*)-**25** was made utilizing (*R, R*)-Me-BPE-Rh.

Evaluation of necroptosis inhibitory activity was performed using a FADD-deficient variant of human Jurkat T cells treated with TNF- $\alpha$  as previously described.<sup>4,10</sup> Utilizing these conditions the cells efficiently underwent necroptosis, which was completely and selectively inhibited by **1** (EC<sub>50</sub> = 0.050  $\mu$ M). For EC<sub>50</sub> value determinations, cells were treated with 10 ng/mL of human TNF- $\alpha$  in the presence of increasing concentration of test compounds for 24 h followed by ATP-based viability assessment.<sup>19</sup>

The initial SAR revealed that the amide NH was crucial for activity. For example, simple methylation (**26** vs **4** and **50** vs **32**) resulted in significant loss of activity. Introduction of branching into the alkyl group at the 4-position of the [1,2,3]thiadiazole increased activity, with *i*-Pr (**31**), *c*-Pr (**32**) and *c*-Bu (**33**) being optimal. However, introduction of a *t*-Bu (**36**) or phenyl (**37**) at this position resulted in decreased activity. The 2-chloro-6-fluoro substitution of the phenyl ring also appeared to be necessary for potent activity. For example, compounds with a 2-methylphenyl (**28**) or 2-methoxyphenyl (**29**) were less active. In addition, the 2,6-dichloro (**38**) or 2,6-difluoro (**39**) substituted derivatives were also less active in some cases compared to 2-chloro-6-fluoro substitution (**32**). Consistent with these findings, removing one of the halogens (**40**) or replacing one of the halogens with small (**41**) or large (**42**) electron-donating groups also resulted in decreased activity. Replacing one of the halogens with other electron-withdrawing groups, such as cyano (**43**) or CF<sub>3</sub> (**44**), did not restore activity. Replacing the 2-chloro-6-fluorophenyl with a 1-naphthyl (**45**), 2-pyridyl (**46**) or substituted 2-pyridyl (**47**) was detrimental to activity. However, addition of a halogen to the 3-position of the 2,6-difluorophenyl (**49**) gave an increase in necroptosis inhibition activity with an EC<sub>50</sub> value of 0.18  $\mu$ M.

Additional changes to the linker between the [1,2,3]thiadiazole and the 2,6-dihalophenyl were also examined (Table 2). The corresponding secondary amine (**14**) and imide (**17**) derivatives of **32** were inactive. Also, the benzylamide was necessary, with the homologous phenethyl amide (**51**) and the truncated anilide (**52**)<sup>20</sup> being significantly less active. Introduction of a methyl group (**53**) onto the benzylic position gave a slight increase in activity. Quite surprisingly, when the two enantiomers of **53** were examined all of the necroptosis activity resided in the (*S*)-enantiomer (**55**). However, increasing the steric bulk of the benzylic substituent to *n*-Bu (**56**), phenyl (**57**) or gem-dimethyl (**58**) resulted in loss of activity.

Finally, modifications to the [1,2,3]thiadiazole heterocycle were examined (Table 3). Replacement with a variety of thiazoles (**59** – **61**) or an oxazole (**62**) was detrimental to activity. Likewise, the pyridazine (**63**), which attempted to replace the sulfur of the [1,2,3]thiadiazole with a CH=CH, was also inactive. However, moderate activity could be obtained with a variety of thiophene derivatives (**64** – **74**), except for the ethoxy derivative **75** and the sulfone derivative **76**. In one cases (**74**) the necroptosis activity approached that seen for the most potent [1,2,3]thiadiazoles. However, replacement of the [1,2,3]thiadiazole with a furan (**77**) was less effective.

In our previous analyses, we discovered that although **1** showed activity in a broad range of necroptosis cellular systems, **2** was restricted to specific cell types/stimuli.<sup>9, 10</sup> For example, **2** efficiently inhibited necroptosis initiated by TNF- $\alpha$  in mouse fibrosarcoma L929 cells, but was ineffective against zVAD.fmk-induced necroptosis in the same cell line.<sup>10</sup> Therefore, a similar analyses with the [1,2,3]thiadiazole series was performed. Compound **55** showed the same activity profile as **2**, providing effective protection of Jurkat or L929 cells from TNF- $\alpha$ -induced necroptosis, while lacking activity in zVAD.fmk treated L929 cells (Figure 2). However unlike **2**, [1,2,3]thiadiazole **55** was fully active in SV40-transformed mouse adult lung fibroblasts stimulated to undergo necroptosis with a combination of TNF- $\alpha$  and zVAD.fmk, in a similar manner to **1**. Collectively, these results demonstrate that the [1,2,3]thiadiazole series poses a distinct mode of necroptosis inhibition compared to the previously

described necrostatins. These data further illustrate that cell-based screening for necrostatins allows for identification of both “universal” (i.e. **1**) and diverse cell type/stimulus specific necroptosis inhibitors (i.e. **2** and **55**). It remains to be determined whether cell type specificity observed *in vitro* translates into *in vivo* models of pathologic injury. If it does, then cell type/stimulus specific inhibitors of necroptosis, such as the tricyclic (i.e. **2**) and the [1,2,3]thiadiazole series (i.e. **55**), may offer advantages under conditions where molecule specificity may be beneficial, such as treating chronic conditions like neurodegenerative diseases.

In conclusion, a series of [1,2,3]thiadiazole benzylamides was found to inhibit TNF- $\alpha$ -induced necroptosis in FADD-deficient variant of human Jurkat T cells. A SAR study revealed that: i) secondary 2,6-dihalo substituted benzylamides were required; ii) when a small alkyl group (i.e. methyl) was present in the benzylic position all the necroptosis inhibitory activity resided with the (*S*)-enantiomer; iii) small branched or cyclic alkyl groups (i.e. *i*-Pr, *c*-Pr or *c*-Bu) were optimal in the 4-position of the [1,2,3]thiadiazole; iv) replacement of the [1,2,3]thiadiazole with a variety of thiophene derivatives was tolerated, although with some erosion of potency. In addition, the [1,2,3]thiadiazole series showed a unique cell type/stimulus necroptosis inhibition profile compared with two previously described classes of inhibitors. Studies are currently underway to evaluate the pharmacology of these compounds in animal models of disease where necroptosis is likely to play a substantial role (i.e. cerebral ischemia, traumatic brain injury and liver injury). Additionally, these compounds are being used to further interrogate the mechanism(s) of necroptotic cell death.

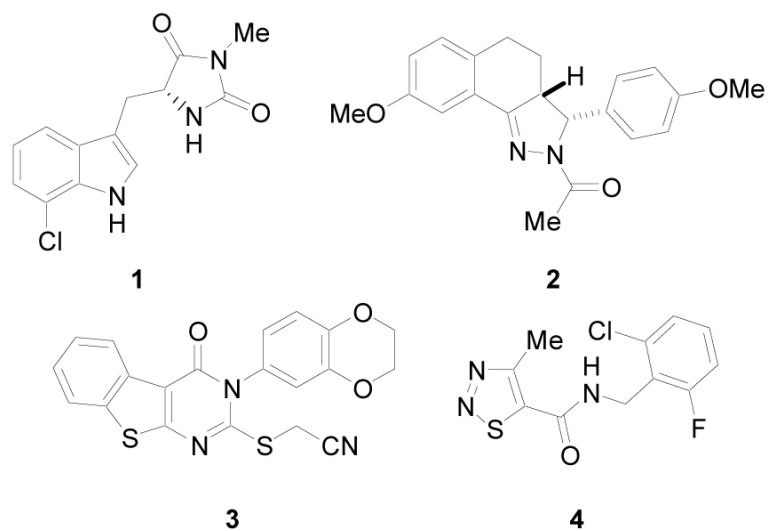
#### Acknowledgements

XT and GDC thank the Harvard Center for Neurodegeneration and Repair (HCNR) for financial support. AD and JY thank the National Institute on Aging, National Institute of General Medical Sciences and American Health Assistance Foundation for financial support. XT, GDC and JY thank the National Institute of Neurological Disorders and Stroke (NINDS) for financial support. JAP Jr. thanks the National Institutes of Health and Bristol-Myers Squibb for financial support. AD is a recipient of NIH Mentored Scientist Development Award from the National Institute on Aging (NIA). The SV40-transformed adult mouse lung fibroblasts were a generous gift of Dr. Philip Tschlis (Tufts University).

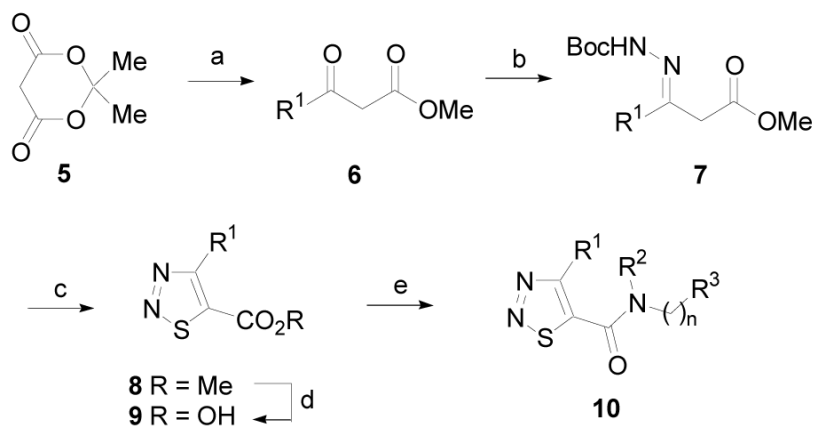
#### References and Notes

1. Wyllie AH, Kerr JFR, Currie AR. *Int. Rev. Cytol* 1980;68:251. [PubMed: 7014501]
2. (a) Cryns V, Yuan J. *Genes & Develop* 1998;12:1551. [PubMed: 9620844] (b) Yuan J, Yankner BA. *Nature* 2000;407:802. [PubMed: 11048732] (c) Talanian RV, Brady KD, Cryns VL. *J. Med. Chem* 2000;43:3351. [PubMed: 10978183] (d) Moore JD, Rothwell NJ, Gibson RM. *Br. J. Pharmacol* 2002;135:1069. [PubMed: 11861336] and references therein (e) Boyce M, Degtrev A, Yuan J. *Cell Death Differ* 2004;11:29. [PubMed: 14647235]
3. (a) Kitanaka C, Kuchino Y. *Cell Death Differ* 1999;6:508. [PubMed: 10381653] For literature related to caspase-independent cell death see: (b) Fiers W, Beyaert R, Declercq W, Vandenabeele P. *Oncogene* 1999;18:7719. [PubMed: 10618712] (c) Borner C, Monney L. *Cell. Death Differ* 1999;6:497. [PubMed: 10381652] (d) Edinger AL, Thompson CB. *Curr. Opin. Cell Biol* 2004;16:663. [PubMed: 15530778] (e) Yu L, Alva A, Su H, Dutt P, Freundt E, Welsh S, Baehrecke EH, Lenardo MJ. *Science* 2004;304:1500. [PubMed: 15131264] (f) Chipuk JE, Green DR. *Nat. Rev. Mol. Cell Biol* 2005;6:268. [PubMed: 15714200] (g) Bröker LE, Kruyt FAE, Giaccone G. *Clin. Cancer Res* 2005;11:3155. [PubMed: 15867207] (h) Fink SL, Cookson BT. *Infect. Immun* 2005;73:1907. [PubMed: 15784530] (i) Kroemer G, Martin SJ. *Nat. Med* 2005;11:725. [PubMed: 16015365] (j) Vandenabeele P, Vanden Berghe T, Festjens N. *Sci. STKE* 2006;358:pe44. [PubMed: 17062895] (k) Martinet W, Schrijvers DM, Herman AG, De Meyer GR. *Autophagy* 2006;2:312. [PubMed: 16874073]
4. Degtrev A, Huang Z, Boyce M, Li Y, Jagtap P, Mizushima N, Cuny GD, Mitchison T, Moskowitz M, Yuan J. *Nat. Chem. Biol* 2005;1:112. [PubMed: 16408008]
5. Martin LJ, Al-Abdulla NA, Brambrink AM, Kirsch JR, Sieber FE, Portera-Cailliau C. *Brain Res. Bull* 1998;46:281. [PubMed: 9671259]
6. Lo EH, Dalkara T, Moskowitz MA. *Nat. Rev. Neurosci* 2003;4:399. [PubMed: 12728267]

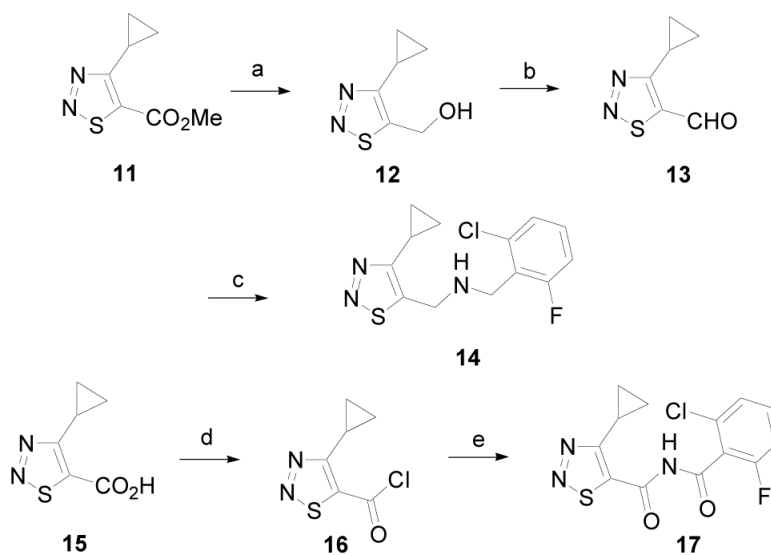
7. McCully JD, Wakiyama H, Hsieh YJ, Jones M, Levitsky S. *Am. J. Physiol. Heart Circ. Physiol* 2004;286:H1923. [PubMed: 14715509]
8. Yuan J, Lipinski M, Degterev A. *Neuron* 2003;40:401. [PubMed: 14556717]
9. Teng X, Degterev A, Jagtap P, Xing X, Choi S, Denu R, Yuan J, Cuny GD. *Bioorg. Med. Chem. Lett* 2005;15:5039. [PubMed: 16153840]
10. Jagtap PG, Degterev A, Choi S, Keys H, Yuan J, Cuny GD. *J. Med. Chem* 2007;50:1886. [PubMed: 17361994]
11. Wang K, Li J, Degterev A, Hsu E, Yuan J, Yuan C. *Bioorg. Med. Chem. Lett* 2007;17:1455. [PubMed: 17270434]
12. Several other biological activities of 4-alkyl-[1,2,3]thiadiazole-5-benzylamides have been reported, including inhibition of I-kappa B kinase complex (IKK), see: Pitts, W.J.; Kempson, J.; Guo, J.; Das, J.; Langevine, C.M.; Spergel, S.H.; Watterson, S.H. WO 2006122137, 2006 and as agents to control plant diseases, see: Umetani, K; Shimaoka, T.; Yamaguchi, M.; Oda, M.; Kyomura, N.; Takemoto, T.; Kikutake, K. WO 2006098128, 2006.
13. Oikawa Y, Sugano K, Yonemitsu O. *J. Org. Chem* 1978;43:2087.
14. Thomas EW, Nishizawa EE, Zimmermann DC, Williams DJ. *J. Med. Chem* 1985;28:442. [PubMed: 3981535]
15. Polniaszek RP, Belmont SE, Alvarez R. *J. Org. Chem* 1990;55:215.
16. Itsuno S, Hachisuka C, Ito K. *J. Chem. Soc., Perkin Trans* 1991;1:1767.
17. Lebel H, Leogane O. *Org. Lett* 2005;7:4107. [PubMed: 16146363]
18. Burk MJ, Wang YM, Lee JR. *J. Am. Chem. Soc* 1996;118:5142.
19. For EC<sub>50</sub> value determinations, FADD-deficient variant of human Jurkat T cells ( $5 \times 10^5$  cells/mL, 100  $\mu$ L per well in a 96-well plate) were treated with 10 ng/mL of human TNF- $\alpha$  in the presence of increasing concentration of test compounds for 24 h at 37 °C in a humidified incubator with 5% CO<sub>2</sub> followed by ATP-based viability assessment. Stock solutions (30 mM) in DMSO were prepared and then diluted with DMSO to give testing solutions, which were added to each test well. The final DMSO concentration was 0.5%. Eleven compound test concentrations (0.030 – 100  $\mu$ M) were used. Each concentration was done in duplicate. Cell viability assessments were performed using a commercial luminescent ATP-based assay kit (CellTiter-Glo) according to the manufacturer's instructions. Cell lysis/ATP detection reagent (40  $\mu$ L) was added to each well. Plates were incubated on a rocking platform for 10 min at room temperature and luminescence was measured using a Wallac Victor 3 plate-reader (Perkin Elmer). Cell viability was expressed as a ratio of the signal in the well treated with TNF- $\alpha$  and compound to the signal in the well treated with compound alone. This was done to account for nonspecific toxicity, which in most cases was < 10%. EC<sub>50</sub> values were calculated using nonlinear regression analysis of sigmoid dose-response (variable slope) curves from plots of log[I] versus viability values.
20. Compound **52** was prepared in low yield (10%) by allowing **16** to react with 2,6-difluoroaniline in THF and pyridine at room temperature. The reaction with 2-chloro-6-fluoroaniline was unsuccessful presumably due to increased steric hindrance.



**Figure 1.**  
Necrostatins

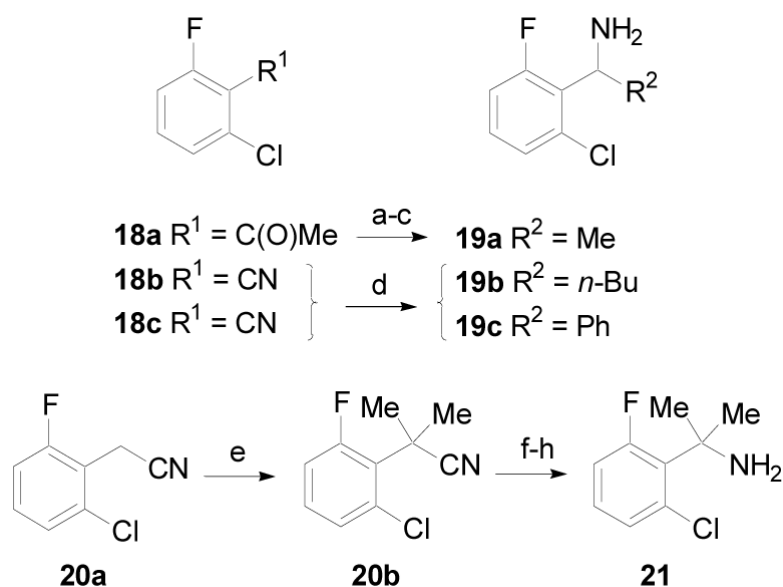
**Scheme 1.**

(a)  $\text{RC(O)Cl}$ , py,  $\text{CH}_2\text{Cl}_2$ , rt, 2 h, then MeOH, 2 h (75%); (b)  $\text{H}_2\text{NNHBoc}$ , cat. TsOH, toluene,  $60^\circ\text{C}$ , 4 h; (c)  $\text{SOCl}_2$ ,  $60^\circ\text{C}$ , 1 h (47% over two steps); (d) 6N HCl, AcOH,  $150^\circ\text{C}$ , 4h; (e) Method A:  $\text{H}_2\text{N}(\text{CH}_2)_n\text{R}^3$ , HBTU,  $i\text{-Pr}_2\text{NEt}$ ,  $\text{CH}_2\text{Cl}_2$ , rt, 12 h (30 – 90%); Method B: oxalyl chloride, cat. DMF,  $\text{CH}_2\text{Cl}_2$ ,  $0^\circ\text{C}$  to rt, 1 h then  $\text{H}_2\text{N}(\text{CH}_2)_n\text{R}^3$ , EtOAc, saturated aqueous  $\text{NaHCO}_3$ , rt, 2 h (20 – 75%); Method C:  $\text{H}_2\text{N}(\text{CH}_2)_n\text{R}^3$ , EDCI, HOBT, DMF, rt, 12 h (60 – 90%).

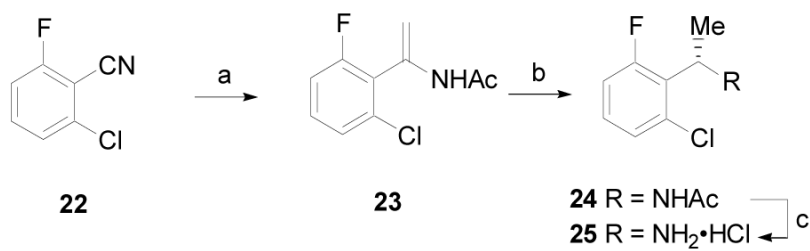
**Scheme 2.**

(a) NaBH<sub>4</sub>, MeOH, rt, 12 h; (b) Dess-Martin reagent, CH<sub>2</sub>Cl<sub>2</sub>, rt, 1 h (65% over two steps); (c) 2-Cl-6-F-PhCH<sub>2</sub>NH<sub>2</sub>, anhydrous MgSO<sub>4</sub>, Et<sub>3</sub>N, THF, rt, 2h then Na(OAc)<sub>3</sub>BH, ClCH<sub>2</sub>CH<sub>2</sub>Cl, rt, 6 h (41%); (d) oxalyl chloride, cat. DMF, CH<sub>2</sub>Cl<sub>2</sub>, 0 °C to rt, 1 h; (e) NaH, 2-Cl-6-F-PhC(=O)NH<sub>2</sub>, THF, rt, 1 h (34% over two steps).

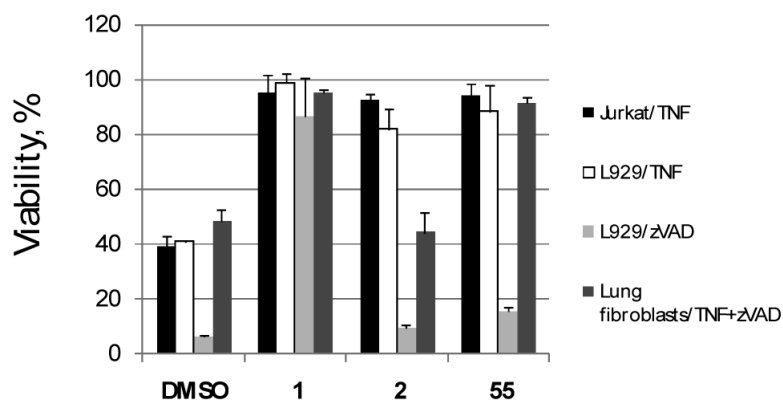


**Scheme 3.**

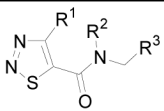
(a) 1M  $\text{BH}_3 \cdot \text{THF}$ , THF, rt, 2 h; (b) diethyl azodicarboxylate,  $\text{PPh}_3$ , phthalimide, THF, rt, 18 h (65 % over two steps); (c)  $\text{H}_2\text{NNH}_2 \cdot \text{H}_2\text{O}$ , THF / EtOH (6:1),  $\Delta$ , 11 h (50%); (d) 1M  $\text{BH}_3 \cdot \text{THF}$ , THF, 0 °C to rt, 1.5 h then  $n\text{-BuLi}$  or  $\text{PhLi}$ , -78 °C, 2 h (15% when  $\text{R}^2 = n\text{-Bu}$ , 20% when  $\text{R}^2 = \text{Ph}$ ); (e)  $\text{NaO-}t\text{-Bu}$ , MeI, NMP, THF, rt, 48 h (85%); (f) 6N HCl, 120 °C, 12 h; (g)  $\text{Boc}_2\text{O}$ ,  $\text{NaN}_3$ ,  $n\text{-Bu}_4\text{NBr}$ , 80 °C, 24 h; (h) TFA, DCM, rt (58% over three steps).

**Scheme 4.**

(a) MeMgCl, THF, rt, 24 h then Ac<sub>2</sub>O, 120 °C, 20 min (43%); (b) (*S,S*)-Me-BPE-Rh (1 mol %), H<sub>2</sub> (60 psi), rt, 12 h (90%); (c) 4N HCl, 120 °C, 6 h (100%).



**Figure 2.** Cell type/stimulus specific activities of necrostatins. FADD-deficient Jurkat, L929 and mouse adult lung fibroblast cells were treated for 24 hr with 10 ng/mL human TNF- $\alpha$  and/or 100  $\mu$ M zVAD.fmk as indicated in the presence of 30  $\mu$ M of necrostatin **1**, **2** or **55**. Cell viability was determined using an ATP-based assessment method. Values were normalized to cells treated with necrostatins in the absence of necroptotic stimulus, which were set as 100% viability. Error bars reflect standard deviation values (N = 2).

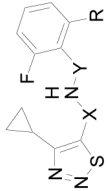
**Table 1**EC<sub>50</sub> determinations of necroptosis inhibition in FADD-deficient Jurkat T cells treated with TNF- $\alpha$ .


The chemical structure shows a thiazole ring with a carbonyl group at the 4-position and a nitrogen substituent at the 5-position. The substituents are labeled R<sup>1</sup>, R<sup>2</sup>, and R<sup>3</sup>.

Compound	R <sup>1</sup>	R <sup>2</sup>	R <sup>3</sup>	EC <sub>50</sub> ( $\mu$ M) <sup>a</sup>
4	Me	H	2-Cl-6-F-Ph	1.0
26	Me	Me	2-Cl-6-F-Ph	11
27	Me	H	2,6-di-F-Ph	3.5
28	Me	H	2-Me-Ph	27
29	Me	H	2-OMe-Ph	> 100
30	<i>n</i> -Pr	H	2-Cl-6-F-Ph	4.1
31	<i>i</i> -Pr	H	2-Cl-6-F-Ph	0.58
32	<i>c</i> -Pr	H	2-Cl-6-F-Ph	0.50
33	<i>c</i> -Bu	H	2-Cl-6-F-Ph	0.60
34	<i>c</i> -Pentyl	H	2-Cl-6-F-Ph	1.9
35	<i>c</i> -Hex	H	2-Cl-6-F-Ph	6.0
36	<i>t</i> -Bu	H	2-Cl-6-F-Ph	18
37	Ph	H	2-Cl-6-F-Ph	> 100
38	<i>c</i> -Pr	H	2,6-di-Cl-Ph	6.0
39	<i>c</i> -Pr	H	2,6-di-F-Ph	1.5
40	<i>c</i> -Pr	H	2-F-Ph	1.5
41	<i>c</i> -Pr	H	2-Cl-6-Me-Ph	10
42	<i>c</i> -Pr	H	2-Cl-6-(OPh)-Ph	> 100
43	<i>c</i> -Pr	H	2-Cl-6-CN-Ph	> 100
44	<i>c</i> -Pr	H	2-F-6-CF <sub>3</sub> -Ph	> 100
45	<i>c</i> -Pr	H	1-naphthyl	> 100
46	<i>c</i> -Pr	H	2-Py	40
47	<i>c</i> -Pr	H	3-F-2-Py	9.6
48	<i>c</i> -Pr	H	2-Cl-3,6-di-F-Ph	0.52
49	<i>c</i> -Pr	H	3-Cl-2,6-di-F-Ph	0.18
50	<i>c</i> -Pr	Me	2-Cl-6-F-Ph	16

<sup>a</sup>Standard deviation < 10%.

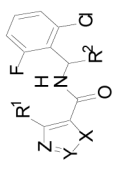
**Table 2**  
 EC<sub>50</sub> determinations of necroptosis inhibition in FADD-deficient Jurkat T cells treated with TNF- $\alpha$ .



Compound	X	Y	R	(R) / (S)	EC <sub>50</sub> ( $\mu$ M) <sup>a</sup>
14	CH <sub>2</sub>	CH <sub>2</sub>	Cl	---	> 100
17	C=O	C=O	Cl	---	> 100
51	C=O	CH <sub>2</sub> CH <sub>2</sub>	Cl	---	27
52	C=O	---	F	---	> 100
53	C=O	CH(Me)	Cl	(R) / (S)	0.40
54	C=O	CH(Me)	Cl	(R)	> 100
55	C=O	CH(Me)	Cl	(S)	0.28
56	C=O	CH( <i>n</i> -Bu)	Cl	(R) / (S)	> 100
57	C=O	CH(Ph)	Cl	(R) / (S)	> 100
58	C=O	C(Me) <sub>2</sub>	Cl	---	> 100

<sup>a</sup> Standard deviation < 10%.

**Table 3**  
 EC<sub>50</sub> determinations of necroptosis inhibition in FADD-deficient Jurkat T cells treated with TNF- $\alpha$ .



Compound	X	Y	Z	R <sup>1</sup>	R <sup>2</sup>	EC <sub>50</sub> ( $\mu$ M) <sup>a</sup>
59	S	CH	N	Me	H	20
60	S	CMe	N	Me	H	> 100
61	S	C(4-ClPh)	N	Me	H	> 100
62	O	CH	N	Me	H	> 100
63	CH=CH	N	N	Me	H	> 100
64	S	CH	CH	Me	H	7.0
65	S	CH	CH	Me	Me	3.9
66	S	CH	CH	Me	H	1.3
67	S	CH	CBr	Me	H	1.2
68	S	CH	CCN	Me	H	5.1
69	S	CH	CH	c-Pr	H	3.9
70	S	CH	CMe	Cl	H	9.6
71	S	CMe	CH	Cl	H	3.9
72	S	CH	CH	H	H	9.4
73	S	CH	CH	H	H	3.7
74	S	CH	CMe	H	H	0.48
75	S	CH	CH	OEt	H	> 100
76	S	CH	CR <sup>3</sup>	Me	H	> 100
77	O	CH	CH	Me	H	13

R<sup>3</sup> = SO<sub>2</sub>-4-Cl-Ph

<sup>a</sup>Standard deviation < 10%.